

AD-A075 365

TECHNICAL
LIBRARY

AD

TECHNICAL REPORT ARBRL-TR-02179

FREE-FLIGHT BASE PRESSURE
MEASUREMENTS ON 8° CONES

Andrew Mark

July 1979



US ARMY ARMAMENT RESEARCH AND DEVELOPMENT COMMAND
BALLISTIC RESEARCH LABORATORY
ABERDEEN PROVING GROUND, MARYLAND

Approved for public release; distribution unlimited.

Destroy this report when it is no longer needed.
Do not return it to the originator.

Secondary distribution of this report by originating
or sponsoring activity is prohibited.

Additional copies of this report may be obtained
from the National Technical Information Service,
U.S. Department of Commerce, Springfield, Virginia
22161.

The findings in this report are not to be construed as
an official Department of the Army position, unless
so designated by other authorized documents.

*The use of trade names or manufacturers' names in this report
does not constitute endorsement of any commercial product.*

UNCLASSIFIED

SECURITY CLASSIFICATION OF THIS PAGE (When Data Entered)

REPORT DOCUMENTATION PAGE		READ INSTRUCTIONS BEFORE COMPLETING FORM
1. REPORT NUMBER TECHNICAL REPORT ARBRL-TR-02179	2. GOVT ACCESSION NO.	3. RECIPIENT'S CATALOG NUMBER
4. TITLE (and Subtitle) FREE-FLIGHT BASE PRESSURE MEASUREMENTS ON 8° CONES		5. TYPE OF REPORT & PERIOD COVERED BRL Report
		6. PERFORMING ORG. REPORT NUMBER
7. AUTHOR(s) Andrew Mark		8. CONTRACT OR GRANT NUMBER(s)
9. PERFORMING ORGANIZATION NAME AND ADDRESS US Army Ballistic Research Laboratory ATTN: DRDAR-BLT Aberdeen Proving Ground, MD 21005		10. PROGRAM ELEMENT, PROJECT, TASK AREA & WORK UNIT NUMBERS 1W662618AH80
11. CONTROLLING OFFICE NAME AND ADDRESS Terminal Ballistics Division US Army Ballistic Research Laboratory Aberdeen Proving Ground, MD 21005		12. REPORT DATE JULY 1979
		13. NUMBER OF PAGES 27
14. MONITORING AGENCY NAME & ADDRESS (if different from Controlling Office)		15. SECURITY CLASS. (of this report) Unclassified
		15a. DECLASSIFICATION/DOWNGRADING SCHEDULE
16. DISTRIBUTION STATEMENT (of this Report) Approved for public release; distribution unlimited.		
17. DISTRIBUTION STATEMENT (of the abstract entered in Block 20, if different from Report)		
18. SUPPLEMENTARY NOTES		
19. KEY WORDS (Continue on reverse side if necessary and identify by block number) Base pressure guns Cones free-flight transducers telemetry		
20. ABSTRACT (Continue on reverse side if necessary and identify by block number) Base pressure measurements are presented on two 8° half angle, right circular cones with a tip bluntness ratio of 1%. Data are obtained at three radial base locations: $r/R_b=0$, $r/R_b=.5$, and $r/R_b=.917$. A unique free-flight technique was employed to obtain the data. The cones were launched nearly vertically from special guns and the data were telemetered to ground stations. The launch Mach numbers were approximately 3 with corresponding Reynolds numbers of 35×10^6 . Both the Mach number and the Reynolds number decreased monotonically		

Item 20.

from their launch value reaching $.04$ and 25×10^4 respectively at apogee. In the laminar flow regime, the centerline base pressure is measured to be a few percent higher than either of the other two. At early times in the trajectory, where the boundary layer was expected to be turbulent, the opposite effect is noted. A crossover in the measured pressures between the center of the base ($r/R_b = 0$) and the outer transducer ($r/R_b = .917$) appears to occur near $M_\infty = 1$. The transducer at $r/R_b = .5$ always indicated a pressure value less than either of the other two.

TABLE OF CONTENTS

	PAGE
LIST OF ILLUSTRATIONS	5
I. INTRODUCTION	7
II. BACKGROUND	7
III. EXPERIMENTAL TECHNIQUE	9
IV. ON-BOARD TELEMETRY AND DATA REDUCTION	13
V. RESULTS AND DISCUSSION	19
REFERENCES	23
LIST OF SYMBOLS	25
DISTRIBUTION LIST	27

LIST OF ILLUSTRATIONS

Figure		Page
1.	8°Half-Angle Cone	10
2.	Cone and Sabot	10
3.	7-inch Smoothbore Launcher	12
4.	9.14 m (30 ft) Smear Camera Photo of 8° Cone in Flight . .	14
5.	15.24 m (50 ft) Smear Camera Photo of 8° Cone in Flight .	14
6.	21.24 m (70 ft) Smear Camera Photo of 8° Cone in Flight .	15
7.	8° Cone and Sabot Parts in Flight	15
8.	Telemetry Data Links	17
9.	Components for the 8° Cone Telemetry System	18
10.	Cone Base Pressure versus Free Stream Mach Number	21
11.	Cone Base Pressure versus Free Stream Reynolds Number . .	22

I. INTRODUCTION

In spite of a great deal of effort expended over the years to guide mathematical models with rational experiments, one of the least understood aerodynamic disciplines has always been base flows of missiles and projectiles. The review and bibliography by Murthy and Osborn¹ of over 700 publications bear witness to this fact. One should not be surprised nor discouraged by this, however, since base aerodynamics must necessarily incorporate all the individual difficult areas of three dimensional viscous and inviscid flows, flows with bodies at angle of attack, and flows with separated regions.

The vast majority of the experimental works have been on sting-supported models paralleled by experiments to describe the sting effect. Comparatively fewer experimenters resort to free-flight techniques for obtaining base pressure data. This results because of a combination of expense and degree of difficulty. Rocket launched vehicles tend to be costly and data are often obtained as a "piggy-back" test on full scale reentry vehicles. Test vehicles free-flighted in wind tunnels must necessarily be small requiring miniaturized telemetry and transducer systems. These also usually require specialized data reduction techniques. Tower drop tests are generally limited to a low Mach number. The clear advantage enjoyed by sting supported models is that their attitude is well controlled. In free-flight, roll and trim control add difficulties in data interpretation and usually result in averaged values or data at angle of attack.

The purpose of this work is to describe base pressure measurements on two 8° half angle cones by means of yet another free-flight technique. The cones were launched from guns at approximately $M_\infty = 3$. Their trajectory was monitored by FPS-16 instrumentation radars and the data were telemetered to ground stations. Continuously varying base pressure data from $M_\infty \approx 3$ to $M_\infty \approx .04$ are therefore obtained corresponding to Reynold numbers of 35×10^6 and 25×10^4 respectively.

II. BACKGROUND

The greatest preponderance of open literature free-flight base pressure data that exists on reentry vehicles has been spawned by the General Electric Company, King of Prussia, Pennsylvania. The major thrust in these efforts has been data gathering in the hypersonic regime.

¹Murthy, S. N. B. and J. R. Osborn, "Base Flow Data with and without Injection: Bibliography and Semi-Rational Correlations," Purdue University, May 1973.

Ianuzzi and Weddington² noted a negative pressure gradient from the base centerline in the laminar regime in wind tunnel free-flight measurements from $M_\infty = 15$ to $M_\infty = 20$. Their experiments were also the first to use a multichannel telemetry system.

Cassanto³ notes a similar negative pressure gradient from the base centerline to $r/R_b = .66$ during a full scale reentry vehicle flight at $M_\infty \approx 20$. The gradient decreases with increasing Reynolds number.

In addition to the radial pressure gradients, Softley and Graber⁴ and Martellucci and Ranlet⁵ noted a local minimum at approximately $r/R_b = .7$ at hypersonic Mach numbers. This trend has also been noted on a sting supported model by Kayser⁶ at supersonic Mach numbers from 1.75 to 4.00.

Cassanto⁷ proposes to use base pressure measurements as a means of inferring pressure profiles of various planets. He also notes certain base pressure characteristics serve as checks for flight performance. For example, at $M_\infty = 1$, a distinct rise in the base pressure is noted. Near $M_\infty \approx 1.2$ a plateau exists where the base pressure is essentially independent of Mach number and Reynolds number.

²Ianuzzi, F. A. and E. D. Weddington, "Free-Flight Base Pressure Measurements across the Base of Sharp and Blunt 10° Cones at Mach Numbers from 15 to 20," AEDC-TR-66-223, December 1966.

³Cassanto, J. M., "Radial Base Pressure Gradients in Laminar Flow," *AIAA Journal*, December 1967.

⁴Softley, E. J. and B. C. Graber, "Techniques for Low Level Pressure and Heat Transfer Measurements and Their Application to Base Flows," General Electric MSD-TIS-R-67SD2, March 1967.

⁵Martellucci, A. and J. Ranlet, "Experimental Study of Near Wakes: Data Presentation," GASL TR-641, March 1967.

⁶Kayser, L. D., "Experimental Study of Separation from the Base of a Cone at Supersonic Speeds," BRL R 1737, August 1974.

⁷Cassanto, J. M., "An Experiment to Determine the Atmospheric Pressure Profile of a Planet using Base Pressure Measurements," AIAA Paper No. 72-202, January 1972.

Pick⁸ obtained free-flight data on a 10° sharp cone in the hypersonic regime and noted that the base pressure was nearly independent between $\alpha = 10^\circ$ and 30° ; showed moderate variation between $\alpha = 0^\circ$ and 10° ; and large variation above $\alpha = 30^\circ$.

III. EXPERIMENTAL TECHNIQUE

Model Description

The 53.67 cm long test vehicles are flat-based, right-circular, 8° half-angle cones with sharp corners and a tip bluntness ratio (R_n/R_b) of 1%. A schematic of the vehicles is shown in Figure 1. The cones are made of hard-coated aluminum with a wall thickness of 1.588 cm. The base is 1.905 cm thick and contains two transducer ports; one at the centerline $r/R_b = 0$, and one at $r/R_b = .5$. These ports were drilled and tapped to accept 10-32 threaded transducers. The third transducer was located at $r/R_b = .917$ and consisted of a .159 cm by 5 cm long port through which pressure was sensed. The base assembly was held in place by a locking ring. The side of the cone contained a slotted opening to accept insertion of the transmitting antenna. In order to make the cone statically stable a weight in the form of a steel tip was added. This piece was threaded and pinned to the aluminum body to insure structural integrity on launch. The steel tip provided a static margin (difference between the center of gravity and the center of pressure) of about .5 cm.

Since the cones are launched from a smoothbore gun, they are supported by a sabot system as the gases propel the vehicle up the tube. The sabot consist of five parts: (1) sabot side petals; (2) obturator; (3) pusher plate; (4) tip support; and (5) gasket. These are shown in Figure 2. The obturator, pusher plate, and side petals interlock to insure that the pieces do not separate while being loaded into the gun. The side petals are machined from a polycarbonate resin and quartered to within 2 cm of the base. They serve as riding surfaces during the vehicle's launch phase. The primary purpose of the polyethelene obturator is to seal the expanding propulsive gases from the vehicle proper. It is designed to be size-on at the forward end and expands with a 1.5° half-angle taper. The length of the obturator is about 8.25 cm. The function of the pusher plate is to transmit a uniform propelling force. It is made from 2.5 cm thick 7075-T6 aluminum. The tip

⁸Pick, G. S., "Base Pressure Distribution on a 10° Sharp Cone at Hypersonic Speeds and High Angles of Attack," AIAA Paper 72-316, April 1972.

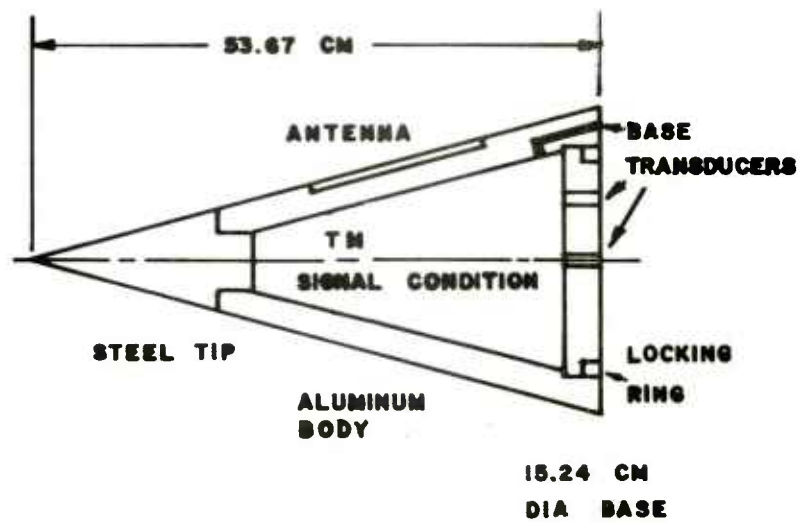


Figure 1. 8° Half-Angle Cone

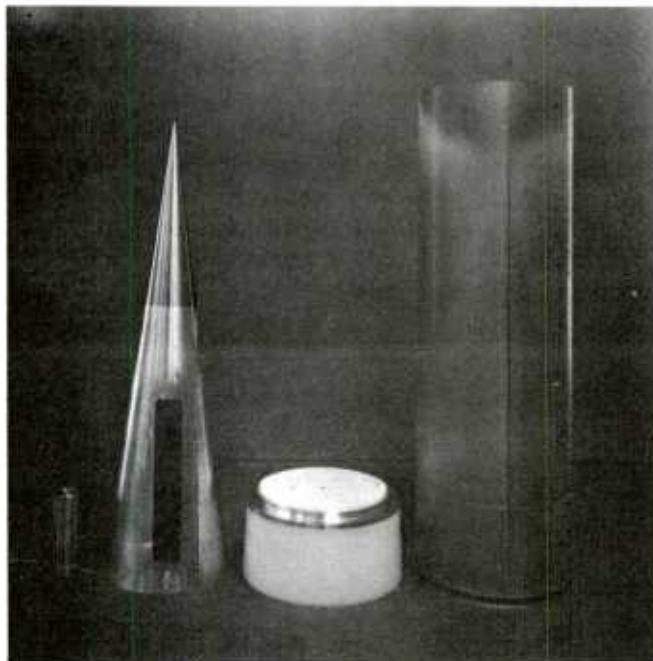


Figure 2. Cone and Sabot

support is the result of an empirical solution to launch failure of similar dual material models in the past. The history of this device goes back over a decade. Typically, the steel nose of a cone projectile would fracture at the threaded joint just after the vehicle exited the tube. It was conjectured to be a rebound effect from the compressive load applied to the system while it was being accelerated up the tube. The tip support is therefore used to absorb the energy in billiard ball fashion that would otherwise be absorbed by the steel nose. The mechanism for the energy absorption and the real cause for failure of the noses without the tip support is unclear. However, it must be said that repeated successful launches are achieved by use of this device. The gasket functions as a seal to prevent propulsive gases from entering the base pressure ports during model compression while accelerating up the tube. Typical propelling pressures can reach 350 MPa whereas the base transducers have a burst pressure of several tenths of a MPa.

Test Site and Instrumentation

The experiments were conducted at the Wallops Island, Virginia, NASA facility. This site is convenient because it has precision instrumentation radars, such as the FPS-16, available for projectile tracking. The FPS-16 has a range precision of ± 4.57 m (RMS) and an angular precision of $\pm .1$ mil (RMS).

The launcher is depicted in Figure 3. The gun is actually made up of two tandemly fitted 7-inch Naval rifles, but welded and reinforced to take the overpressure. It is approximately 85 calibers long. It has the capability of being raised to any elevation between 0° and 90° from the horizontal. Our particular firing elevation was 80° . The launcher is surveyed into position and directed to fire on an azimuth of 130° from TN. Vehicle recovery is not attempted since the beach firing site and launch azimuth cause it to fall into the sea. This gun, one of several in existence, has better than a $M_\infty = 6$ capability and has attained altitudes of 180 km with low drag shapes weighing approximately 23 kg. A 16" version of the same system can propel a 180 kg payload to a $M_\infty = 9$ muzzle velocity.

The FPS-16 radar trajectory, together with rawinsonde atmospheric data, allow us to reconstruct the vehicle Reynolds number history. Maximum error in the precision of rawinsonde temperature and pressure data is about .3% over sea level to 5200 m altitude. The corresponding one standard deviation is approximately .08% for both sets of data.

Three smear cameras were used to photograph the projectile and sabot parts at 9.14 m (30ft), 15.24 m (50 ft), and 21.34 m (70 ft) from the muzzle. Photographs of one of the launches are shown in



Figure 3. 7-inch Smoothbore Launcher

Figures 4, 5, and 6. This gives the reader an idea of the muzzle environment experienced by the vehicles. Some of the sabot parts can be identified in these photographs. The white regions in Figures 4 and 5 are either hot gases or burning sabot pieces. In Figure 4 the tip of the cone is clearly seen protruding from the cloud. In Figure 6 only the cone, the pusher plate, the two tip support halves, and a partial gasket are seen. The rest of the sabot components are out of the field of view. A fourth smear camera (Figure 7) angled slightly from behind gives a wider field of view of the same event. This camera is pointed at approximately the 21.34 m (70 ft) position and serves only to view the sabot pieces as they separate from the vehicle.

The purpose of the cameras is twofold: (1) they allow one to view catastrophic model failure, and (2) the three precisely located smear cameras together with a framing camera aimed at the muzzle, allow one to infer the muzzle velocity of the test vehicle. This is done by imprinting a common time trace on all cameras and resolving distance-time differences. The muzzle velocities thusly obtained were compared to an independent measurement system consisting of a radar doppler velocimeter. The initial velocities from these two techniques agreed to within less than one percent of each other. It is important that this velocity be known accurately since the FPS-16 radars typically lock on the vehicle several seconds after launch. The initial portion of the trajectory (the first five seconds in our case) is simulated with a computed point mass trajectory by knowing the initial velocity and the matching velocity at radar acquisition. By adjusting the cone yaw over the early part of the trajectory (i.e., the drag history) a better than one percent match in velocity and position at radar acquisition is achieved.

The Wallops Island Facility also supplied us with two fixed telemetry receiving stations. Each uses a 3.65 m parabolic, 28 db gain antenna feeding Defense Electronics Incorporated TMR-74B receivers. Since these telemetry stations are in defilade with respect to the firing site (and 25 km away), a Ballistic Research Laboratory Mobile Station was used to obtain data near the muzzle.

IV. ON-BOARD TELEMETRY AND DATA REDUCTION

The transducer used for these tests were commercially available from Kulite and had a range of 1 atm. These types of transducers had previously survived the high-g launch of gun systems. Typical launch acceleration for the 7-inch gun at $M_\infty = 3$ is approximately 27,000 g with a duration of about 20 ms. Not only must the transducers survive the launch acceleration but gun gases, with pressures exceeding 200 MPa (30,000 psi), must not contact the transducers since this high pressure would easily rupture the diaphragms. This

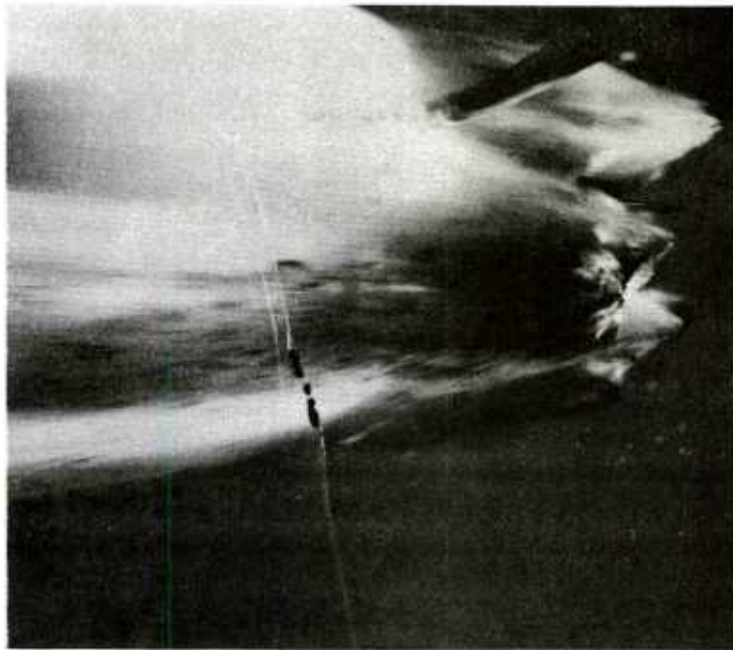


Figure 4. 9.14 m (30 ft) Smear Camera
Photo of 8° Cone in Flight



Figure 5. 15.24 m (50 ft) Smear Camera
Photo of 8° Cone in Flight

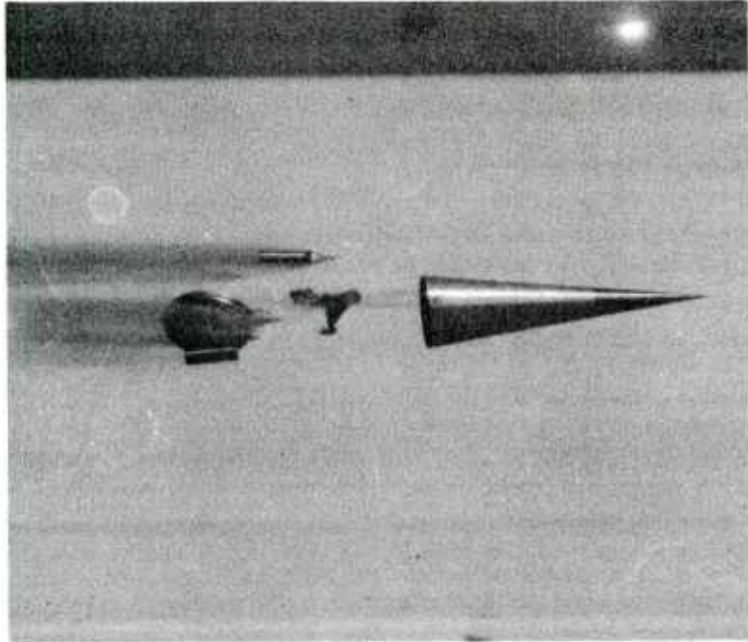


Figure 6. 21.24 m (70 ft) Smear Camera
Photo of 8° Cone in Flight

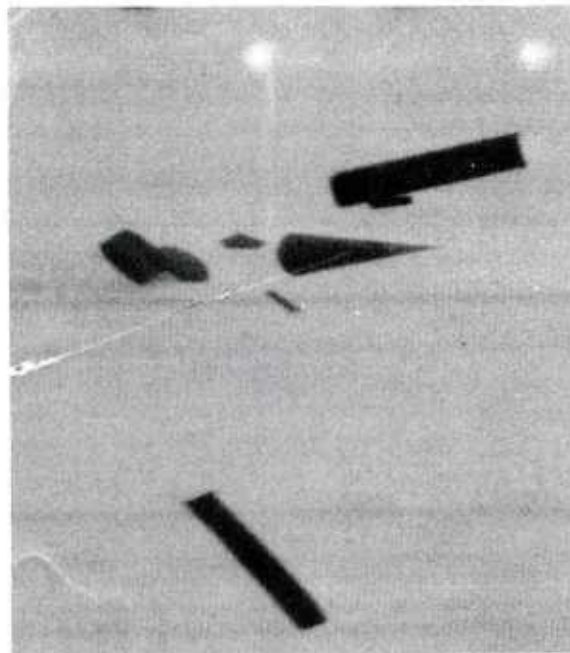


Figure 7. 8° Cone and Sabot Parts in Flight

is the reason the polyethelene gasket is used between the base of the cone and the pusher plate. As the vehicle is accelerating in the tube, a compressive action seals off any access gun gases might have to the transducers.

A schematic of the telemetry data links, including the data reductions system, is shown in Figure 8. Each transducer was amplified and in turn sampled by a 32 channel electronic commutator. The commutator frequency was 3200 Hz or 100 frames/s. The output of the commutator drove a standard IRIG 93 KHz, $\pm 15\%$ deviation, subcarrier oscillator which in turn modulated a 250 MHz transmitter. The power of the transmitter was between 100 and 200 mw and radiated through a slot antenna in the side of the cone as depicted in Figure 9. From this photograph one can also get an idea of the size of the various parts involved. By far the biggest bulk is in the Nickel-Cadmium batteries. A potting resin is poured into the cone under vacuum after the electronic components are installed.

When the signal is intercepted by the receiving antenna, the subcarrier oscillator modulated by the commutator is recorded on tape. The signal appears as a time varying frequency (center portion of Figure 8). The tape may now be played back at leisure through a discriminator to recover the commutated signal. This may be displayed on a scope, strip chart, etc. In view of the large quantity of data, the commutated signal was A/D converted with a sampling rate of 32 KHz. This meant that each channel of the commutator contained 10 sample points. The data are now in a form to be automatically reduced by a computer. This was done on BRL's CDC 7600. It should be pointed out that some of the commutator channels were allocated for reference signals. A built-in calibrator served to check 0v, 5v, and 2.5v for each frame. Additionally, we used divider circuits to monitor battery voltage and regulated voltage at the transducers, amplifier, commutator, subcarrier oscillator, and transmitter.

Data Accuracy

The system was final calibrated once all the electronics were installed and potting had been allowed to set. Pressure calibration below one atmosphere was accomplished by a manometer with an accuracy better than 1 part per 1000. Transducer linearity was better than .25% through the complete system. The A/D was readable to 1 part in 2079. The transducers were temperature compensated from -18°C ($\approx 0^{\circ}\text{F}$) to $+38^{\circ}\text{C}$ ($\approx 100^{\circ}\text{F}$). These units typically have a thermal sensitivity coefficient of 2 to 3% per 55°C . Our temperature excursions were much less than this. Therefore, taking into account calibration through the telemetry system, linearity of the system to the A/D conversion, the conversion itself, and thermal effects, it is expected that the base pressure is accurate to about 1%.

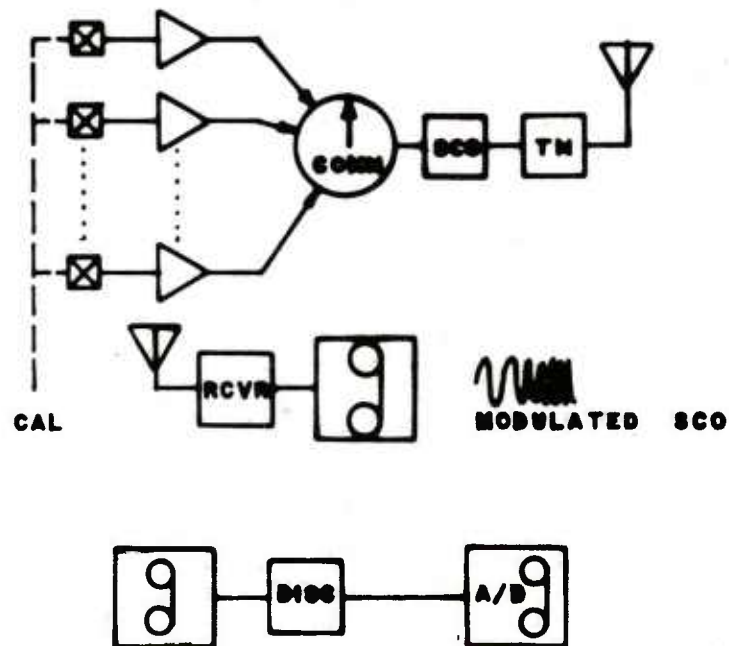


Figure 8. Telemetry Data Links

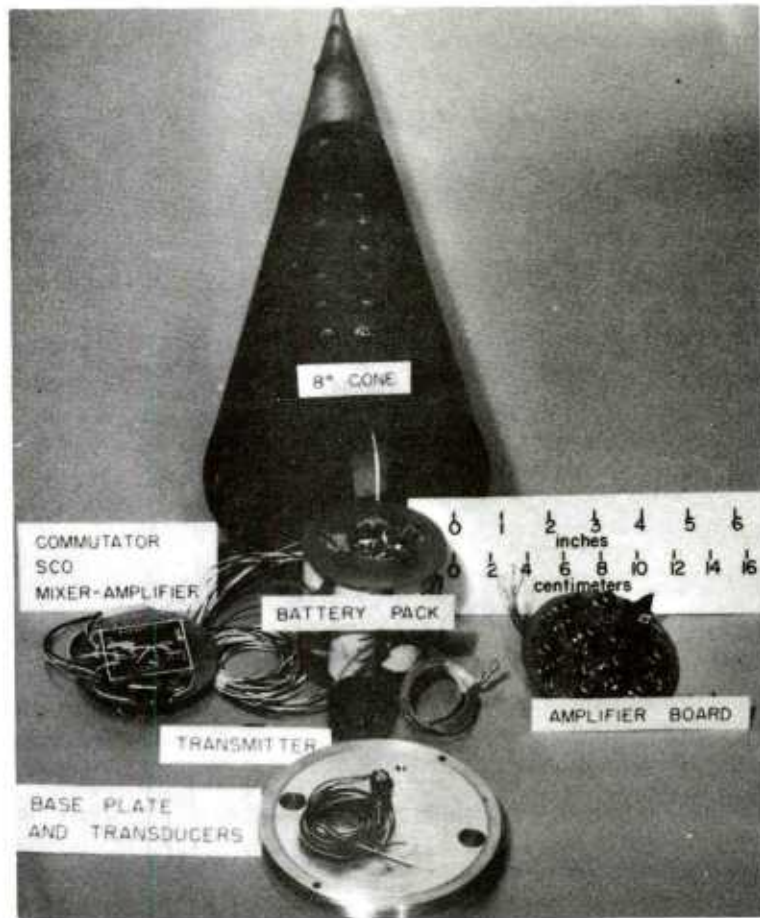


Figure 9. Components for the 8° Cone Telemetry System

The accuracy of the inferred Mach numbers and Reynolds numbers depends largely on the accuracy of the velocity history and to a lesser degree on the atmospheric thermal profile measurement. The position accuracy of the FPS-16 radar dictates 1 part per several thousand; i.e. less than 1%. However when differentiating the smoothed position-time data to obtain velocity, RMS errors of several percent are obtained. These, combined with the fact that the early portion of the trajectory is computed, suggests that the overall velocity history, and indeed the Mach number and Reynolds number history, attain errors of approximately 5%.

As mentioned previously, rawinsonde RMS accuracies in temperature and atmospheric pressure are approximately .08% and as such are a minor influence on the Mach number and Reynolds number.

V. RESULTS AND DISCUSSION

The average base pressure results for the two 8° half-angle cone flights (8456 and 8459) are summarized in Figures 10 and 11. The Reynolds number in these two figures is based on wetted length and free stream conditions. For flight 8456 only the $r/R_b = .5$ transducer functioned whereas the other two transducers functioned for flight 8459. It is impossible to tell what caused their failure. Therefore Figures 10 and 11 represent composites from the two flights. Figure 10 shows the distribution of base pressure as a function of Mach number and Figure 11 as a function of Reynolds number. It should be noted that although average values of base pressure are presented, some oscillation in the vehicles and therefore necessarily in the data, did occur. Both rounds exhibited about a 5° maximum angle of attack just after exiting the muzzle but damped to near $\alpha = 0^\circ$ within one or two seconds. At approximately 10 seconds both rounds experienced fairly large angular perturbations (11° - 13°) and damped in two to three seconds. It is difficult to know exactly what caused this maneuver. The conjecture is that transition occurred on the model. The Reynolds number, based on free stream properties, for this event is 4.5×10^6 . According to Pate,⁹ transition based on local conditions occurs at a Reynolds number of about 4×10^6 . Since at that time in our flight the vehicle was at $M_\infty \approx .6$, the local Reynolds number conditions would have been nearly the same as the free stream Reynolds number and transition is thus implied. The transition Reynolds number changes drastically with angle of attack

⁹Pate, S.R., "Measurements and Correlations of Transition Reynolds Number on Sharp Slender Cones at High Speeds," AEDC-TR-69-172, December 1966.

as noted by Schmidt and Cresci¹⁰ as a result of cross flows and vortex shedding. They noted a leeside turbulent flow while the windward side remained laminar. It is possible that asymmetric separation caused the vehicles to oscillate.

The base pressure plateau, as mentioned by Cassanto⁷ is very well defined in both Figures 10 and 11. In Figure 10 it occurs between $M_\infty = 1$ and $M_\infty = 1.25$. All three transducers seem to exhibit this characteristic. The corresponding Reynolds number for this occurrence is between 13×10^6 and 16×10^6 based on free stream conditions. The 30% jump in the base pressure at $M_\infty = 1$ is noted by Somer and Yee¹¹ and Cassanto and Buce¹². Cassanto⁷ advocates using both these facts as benchmarks for mapping trajectories and atmospheric pressures on planetary probes.

Direct comparison with data of other authors is not possible because of the range of variables considered. The free flight tests described in this work cover a much wider range of Mach numbers and Reynolds numbers than has ever been considered before. Previous free-flight experiments were performed in wind tunnels where flight times were of the order of milliseconds. They usually simulated high altitude (low Reynolds number) flights at a very limited range of Mach numbers. Additionally, some of the full scale reentry vehicle flights attained high Reynolds numbers but at Mach numbers near 20. The present measurements are a first attempt to obtain continuous Mach number and Reynolds number data at low altitude and so only trends be compared with other authors.

The radial pressure gradients noted by Cassanto³ in laminar flow at $M_\infty \approx 20$ are not evident at the lower Mach number. In this experiment only about a 10% variation was detected. However, the direction was qualitatively the same, i.e., the pressure at the centerline was higher than near the base edge. The data also show a coalescing of the pressures near $M_\infty = .1$ (large $Re_{l,\infty}$) implying that the lesser pressure now exists at model centerline. (See inset to Figure 11). The variation is still small ($\approx 10\%$) and has not been demonstrated to be significant. At higher Reynolds numbers the base gradient effect is consistently shown to be minimal by other authors⁷.

¹⁰Schmidt, E. M. and R. J. Cresci, "Near Wake of a Slender Cone in Hypersonic Flow," AGARD Conference on Fluid Physics of Hypersonic Wakes, vol. 1, May 1967.

¹¹Sommer, S. and L. Yee, "An Experiment to Determine the Structure of a Planetary Atmosphere," AIAA Paper No. 68-1054, October 1968.

¹²Cassanto, J.M. and P. Buce, "Free Fall Drop Tests to Determine Low Speed Stability and Base Pressure Characteristics for Blunt Planetary Entry Bodies," JSR, Vol. 8 No. 7, July 1971.

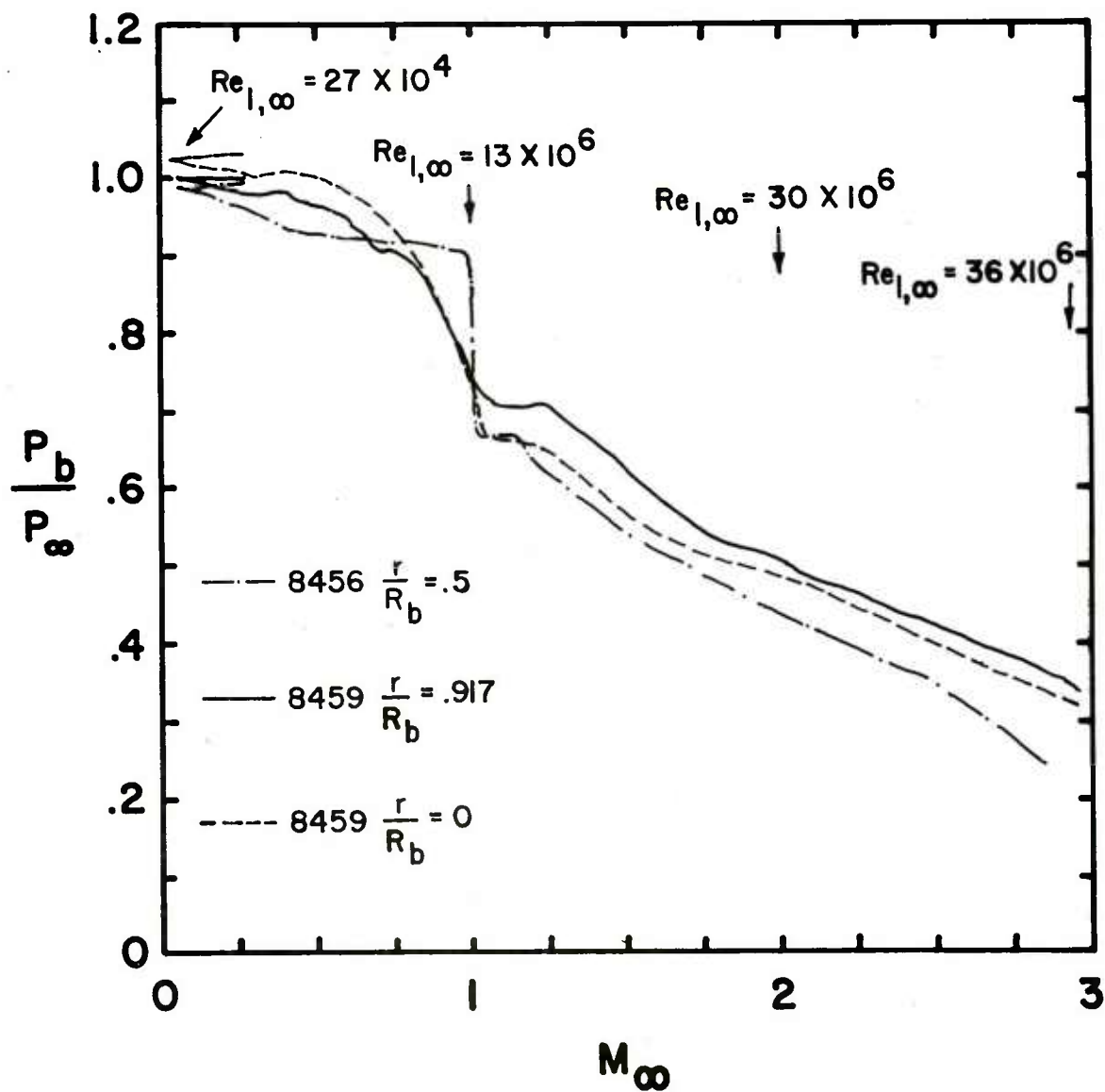


Figure 10. Cone Base Pressure versus Free Stream Mach Number

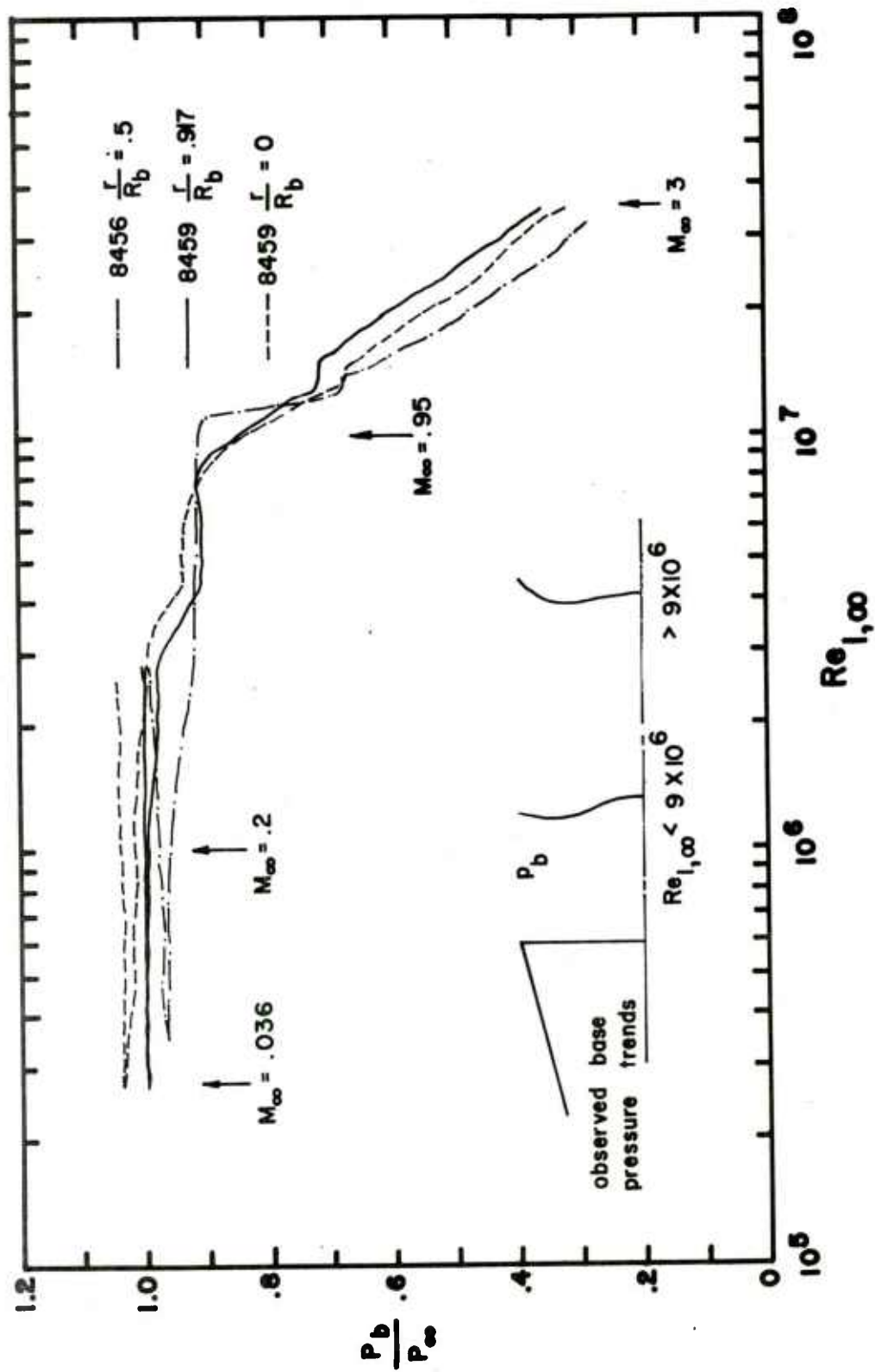


Figure 11. Cone Base Pressure versus Free Stream Reynolds Number

REFERENCES

1. Murthy, S. N. B. and J. R. Osborn, "Base Flow Data with and without Injection: Bibliography and Semi-Rational Correlations," Prudue University, May 1973
2. Ianuzzi, F. A. and E. D. Weddington, "Free-Flight Base Pressure Measurements across the Base of Sharp and Blunt 10° Cones at Mach Numbers from 15 to 20," AEDC-TR-66-223, December 1966.
3. Cassanto, J. M., "Radial Base Pressure Gradients in Laminar Flow," AIAA Journal, December 1967.
4. Softley, E. J. and B. C. Graber, "Techniques for Low Level Pressure and Heat Transfer Measurements and Thin Application to Base Flows," General Electric MSD-TIS-R-67SD2, March 1967.
5. Martellucci, A. and J. Ranlet, "Experimental Study of Near Wakes: Data Presentation," GASL TR-641, March 1967.
6. Kayser, L. D., "Experimental Study of Separation from the Base of a Cone of Supersonic Speeds," BRL R 1737, August 1974. (AD #A005015)
7. Cassanto, J. M., "An Experiment to Determine the Atmospheric Pressure Profile of a Planet using Base Pressure Measurements," AIAA Paper No. 72-202, January 1972.
8. Pick, G. S., "Base Pressure Distribution of a 10° Sharp Cone at Hypersonic Speeds and High Angles of Attack," AIAA Paper No. 72-316, April 1972.
9. Pate, S. R., "Measurements and Correlations of Transition Reynolds Number on Sharp Slender Cones at High Speeds," AEDC-TR-69-172, December 1966
10. Schmidt, E. M. and R. J. Cresci, "Near Wake of a Slender Cone in Hypersonic Flow," AGARD Conference on Fluid Physics of Hypersonic Wakes, vol. 1, May 1967.
11. Sommer, S. and L. Yee, "An Experiment to Determine the Structure of a Planetary Atmosphere," AIAA Paper No. 68-1054, October 1968.
12. Cassanto, J.M. and P. Buce, "Free Fall Drop Tests to Determine Low Speed Stability and Base Pressure Characteristics for Blunt Planetary Entry Bodies," JSR, Vol. 8, No. 7, July 1971.

LIST OF SYMBOLS

d	base diameter (m)
L	model length along symmetry axis (m)
M	local Mach number
M_{∞}	free stream Mach number
p_b	base pressure (Pa)
p_{∞}	free stream static pressure (Pa)
r	radial distance from model centerline (m)
R_b	base radius (m)
R_n	nose radius (m)
$Re_{\ell, \infty}$	Reynolds number based on wetted length and free stream conditions
t	time (s)
α	angle of attack (deg)
θ_c	cone half angle (deg)

DISTRIBUTION LIST

<u>No. of Copies</u>	<u>Organization</u>	<u>No. of Copies</u>	<u>Organization</u>
12	Commander Defense Documentation Center ATTN: DDC-DDA Cameron Station Alexandria, VA 22314	2	Commander US Army Missile Research and Development Command ATTN: DRDMI-R DRDMI-YDL Redstone Arsenal, AL 35809
1	Commander US Army Materiel Development and Readiness Command ATTN: DRCDMD-ST 5001 Eisenhower Avenue Alexandria, VA 22333	1	Commander US Army Tank Automotive Rsch and Development Command ATTN: DRDTA-UL Warren, MI 48090
1	Commander US Army Aviation Research and Development Command ATTN: DRSAB-E P.O. Box 209 St. Louis, MO 63166	2	Commander US Army Armament Research and Development Command ATTN: DRDAR-TSS Dover, NJ 07801
1	Director US Army Air Mobility Research and Development Laboratory Ames Research Center Moffett Field, CA 94035	1	Commander US Army Armament Materiel Readiness Command ATTN: DRSAR-LEP-L, Tech Lib Rock Island, IL 61299
1	Commander US Army Electronics Research and Development Command Technical Support Activity ATTN: DELSD-L Fort Monmouth, NJ 07703	1	Director US Army TRADOC Systems Analysis Activity ATTN: ATAA-SL, Tech Lib White Sands Missile Range NM 88002
1	Commander US Army Communications Rsch and Development Command ATTN: DRDCO-PPA-SA Fort Monmouth, NJ 07703		<u>Aberdeen Proving Ground</u> Dir, USAMSAA ATTN: Dr. J. Sperrazza DRXSY-MP, H. Cohen Cdr, USATECOM ATTN: DRSTE-TO-F Dir, Wpns Sys Concepts Team, Bldg. E3516, EA ATTN: DRDAR-ACW

USER EVALUATION OF REPORT

Please take a few minutes to answer the questions below; tear out this sheet and return it to Director, US Army Ballistic Research Laboratory, ARRADCOM, ATTN: DRDAR-TSB, Aberdeen Proving Ground, Maryland 21005. Your comments will provide us with information for improving future reports.

1. BRL Report Number _____
2. Does this report satisfy a need? (Comment on purpose, related project, or other area of interest for which report will be used.)

3. How, specifically, is the report being used? (Information source, design data or procedure, management procedure, source of ideas, etc.) _____

4. Has the information in this report led to any quantitative savings as far as man-hours/contract dollars saved, operating costs avoided, efficiencies achieved, etc.? If so, please elaborate.

5. General Comments (Indicate what you think should be changed to make this report and future reports of this type more responsive to your needs, more usable, improve readability, etc.) _____

6. If you would like to be contacted by the personnel who prepared this report to raise specific questions or discuss the topic, please fill in the following information.

Name: _____

Telephone Number: _____

Organization Address: _____

